

$^1\text{H}/^{19}\text{F}$ MRI of Lung Angiogenesis with $\alpha_v\beta_3$ -integrin Targeted Perfluorocarbon Nanoparticles

Anne Schmieder¹, Shelton Caruthers¹, John Stacy Allen¹, Todd Williams¹, Elizabeth Wagner², Samuel Wickline¹, and Gregory Lanza¹
¹Washington University Medical School, St Louis, MO, United States, ²Johns Hopkins University, Baltimore, MD, United States

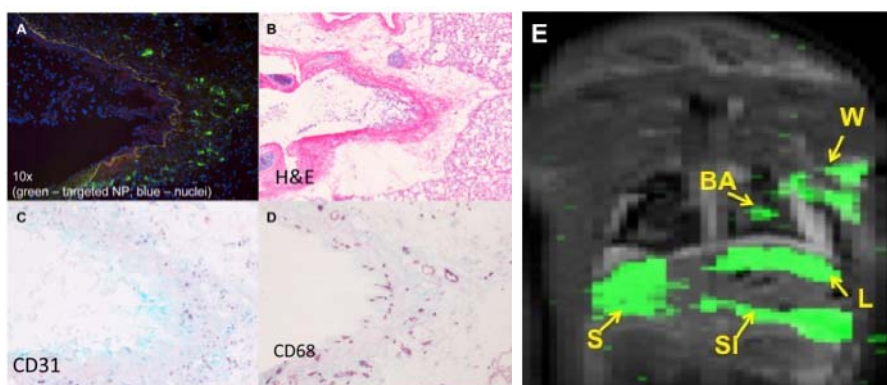
Introduction: Asthma is a chronic inflammatory lung disease that affects an estimated 25 million Americans (7 million children). The symptoms of asthma cause significant economic burden on the healthcare systems (\$18B in 2008) as well as dramatic impact on the quality of patients' lives. Recently, the long recognized increase in airway wall microvessel density and expanded blood volume associated with asthma have been suggested to contribute significantly to airway obstruction and decreased lung function [1]. We have previously shown MR imaging of angiogenesis in several animal models by targeting the neovascular biomarker $\alpha_v\beta_3$ -integrin, which is upregulated on proliferating versus quiescent endothelial cells [2-4]. We hypothesized that $\alpha_v\beta_3$ -integrin targeted perfluorocarbon nanoparticles may be used for high resolution, dual $^1\text{H}/^{19}\text{F}$ 3D MR molecular imaging at 3T for noninvasive characterization of bronchial angiogenesis.

Methods: Perfluorocarbon (PFC) nanoparticles (NPs) were prepared as previously described [5]: 20% (v/v) perfluorooctylbromide (PFOB, Exflur Inc., Round Rock, TX), 2.0% (w/v) of a surfactant co-mixture, and 1.7% (w/v) glycerin in pH 6.5 carbonate buffer. The surfactant co-mixture of the NPs consisted of ~98 mole% lecithin, 1.7 mole% phosphatidylethanolamine (PE), 0.2 mole% AlexaFluor488 (Invitrogen) coupled to PE, and 0.1 mole % of a peptidomimetic $\alpha_v\beta_3$ -integrin antagonist[6]. The surfactant components were combined with the PFOB, buffer, and glycerin with pH adjusted to 6.5, and the mixtures were emulsified. Nominal particle sizes measured by dynamic light scattering was ~200 nm with a polydispersity of ~0.2 (Brookhaven Instrument Corp.) A left pulmonary artery ligation (LPAL) model of inflammation-induced angiogenesis was used to study the bronchial artery proliferation in rats by MR. The response to pulmonary ischemia in the rat most closely resembles bronchial neovascularization in human subjects after pulmonary artery obstruction [7]. Briefly, in anesthetized, ventilated rats, a left thoracotomy was performed through the 3rd intercostal space and ribs separated for exposure. Under microscopic visualization, the LPA was dissected from the airway, ligated, the ribs and skin were opposed, and the wound sutured. Three days following LPAL, rats (n=5) were administered $\alpha_v\beta_3$ -targeted PFOB NPs (1.0 ml i.v./kg). After allowing the NPs to circulate for 2 hours, rats were sacrificed and imaged with high-resolution $^1\text{H}/^{19}\text{F}$ MRI to characterize the spatial distribution of bronchial angiogenesis. Images were acquired at 3T (Philips Achieva) using an in-house, custom dual-tuned open birdcage transmit-receive coil. Simultaneous 3D $^1\text{H}/^{19}\text{F}$ imaging was used employing a novel steady state (aka, 'balanced') ultrashort echo time (UTE) technique (TE/TR=0.1ms/1.96ms) with the frequencies set to the resonance of ^1H and the CF_2 groups of the PFOB spectrum (representing 12 of 17 total ^{19}F nuclei)[8]. Using a highly oversampled 3D radial readout scheme, the reconstructed image datasets have a nominal resolution of 1.25x1.25x1.25 mm³, but can be reconstructed, post facto, at lower resolutions if required to optimize the signal-to-noise ratio (SNR). Typical total scan time was 28min.

Results: Fluorine images were reconstructed offline at a range of resolutions to maximize SNR. Fluorine signal located in the left lung was obvious for all animals and was minimal in the uninjured right lung. A representative image is shown in Fig. 1. The fluorine signal on the MR images revealed the marked expansion of angiogenesis at the left thoracotomy wound site and the left mediastinal lung where the LPA was occluded. Other prominent sites of signal were appreciated in the spleen, liver and intestine, associated with reticuloendothelial clearance and biliary

excretion. As shown in panels A-D, angiogenesis targeting in the lung was corroborated histopathologically using fluorescent-labeled $\alpha_v\beta_3$ -targeted PFC NPs.

Fig 1. *A.* $\alpha_v\beta_3$ -targeted PFC NP with AF488 (green) targeted near airway (*B*, H&E) associated with neovessel proliferation (*C*, CD31) and increased inflammatory macrophages (*D*, CD68). *E.* $^1\text{H}/^{19}\text{F}$ 3T MR coronal slice showing angiogenesis expressed in the thoracotomy wound (W) and bronchial angiogenesis (BA). Negligible signal was seen in the right, uninjured lung. NP clearance was appreciated in the liver (L), spleen (S), and small intestine (SI).



Conclusion: In this study, we have used a novel application of dual $^1\text{H}/^{19}\text{F}$ MR molecular imaging with a clinical 3T scanner to noninvasively image bronchial angiogenesis. The unique k-space data acquisition techniques employed supported multi-resolution, multi-sensitivity retrospective reconstruction of the simultaneously acquired $^1\text{H}/^{19}\text{F}$ data. This molecular imaging approach to asthma employs quantitative image stratification to assess the temporal-spatial changes in airway vascularity, and has the potential to deliver acute antiangiogenic nanotherapy in conjunction with current standard of care drugs to offer a clinically translatable approach to ameliorate the progression of moderate to severe asthma ultimately to reduce hospitalizations and home health-care costs.

1. Voelkel, N.F. et al., Immunol Cell Biol, 2009
3. Schmieder, A.H., et al., Magn Reson Med, 2005.
5. Flacke, S., et al., Circulation, 2001.
7. Endryns, J., et al., Heart, 1997.

2. Winter, P.M., et al., Cancer Res, 2003.
4. Winter, P.M., et al., Circulation, 2003.
6. Meoli, D.F., et al., J Clin Invest, 2004.
8. Keupp J., et al., Proc. Intl. Soc. Magn. Reson. Med., 2011(#2828).